 

PACS numbers: 42.65.Jx; 42.65.Re; 52.50.Jm
DOI: 10.1070/QE2014v044n06ABEH015453

# Filamentation of a phase-modulated pulse under conditions of normal, anomalous and zero group velocity dispersion

S.V. Chekalin, E.O. Smetanina, A.I. Spirkov, V.O. Kompanets, V.P.Kandidov

*Abstract.* **We have investigated experimentally and numerically the influence of the initial temporal phase modulation of a pulse on the spatiotemporal intensity distribution and the frequency-angular spectrum of femtosecond laser pulses with self-channelling in a condensed medium. We have detected a decrease in the intensity of divergent anti-Stokes frequency components during filamentation of radiation under conditions of normal group-velocity dispersion (GVD) and strong phase modulation. In the zero-GVD regime under conditions of the phase modulation of radiation, the spatiotemporal transformation of the pulse is similar to that in the normal-GVD regime, which leads to a qualitative change in the supercontinuum spectrum. In the anomalous-GVD regime, a sequence of 'light bullets' is formed in the filament for both a phase-modulated and a transform-limited pulse.**

***Keywords:*** *filamentation, femtosecond pulses, anomalous dispersion, plasma channels, light bullets.*

## 1. Introduction

The formation of an extended filament with strong field localisation of energy by femtosecond laser radiation is the result of the dynamic balance of Kerr self-focusing of radiation in a medium and its defocusing in an induced laser plasma [1–3]. The material dispersion of a medium has a significant influence on the formation of filaments and the spatiotemporal intensity distribution in the process of filamentation [4]. In the region of normal group-velocity dispersion (GVD) the pulse splits into subpulses, and in the region of zero GVD there occurs multiple Kerr self-focusing of the pulse tail that has experienced defocusing in a self-induced laser plasma [5]. In the anomalous-GVD regime, a sequence of 'light bullets' is formed, i.e., areas of quasi-periodic optical field localisation in space and time [6, 7].

Phase modulation of radiation enables a control of such parameters as the filament start and length, the efficiency of supercontinuum generation and pulse compression [8–10]. Compensation for the pulse dispersion spreading in air by negative linear phase modulation of radiation at the centre wavelength $\lambda_0$ = 800 nm has made it possible to design a broadband coherent source in a filament at a height of more than 10 km [11] and to improve the efficiency of supercontinuum generation [12]. By using temporally chirped femtosecond Bessel–Gaussian beams in air, Polynkin et al. [13] detected less bright rings of conical emission and a stronger on-axis supercontinuum emission intensity than for a transform-limited pulse having the same profile [13]. Under normal GVD in a condensed medium (ZK7 glass) the negative phase modulation of the pulse leads to the regime of filamentation with a low concentration of a self-induced laser plasma and, hence, to the disappearance of conical supercontinuum emission [14]. In noble gases, the phase modulation is used to obtain few-cycle pulses during filamentation [15, 16]. The negative pulse phase modulation can be employed to suppress small-scale filamentation under atmospheric turbulence conditions [17, 18] and also to increase the self-induced laser plasma density [19].

All the above-mentioned works were carried out under conditions of normal GVD in a medium. This paper presents the results of experimental and numerical study of filamentation in the normal-, zero- and anomalous-GVD regimes for pulses with a linear frequency positive and negative phase modulation (chirp). The effect of the phase modulation of the pulse on filamentation in various GVD regimes is considered for fused silica, where the spatial scales are smaller and the dispersion effects are much stronger than those in air. For example, at $\lambda_0$ = 800 nm the $k_2$ parameter defining GVD is equal to 0.2 fs$^2$ cm$^{-1}$ in air, whereas it is ~360 fs$^2$ cm$^{-1}$ in fused silica [20, 21]. This allowed us to study in detail under laboratory conditions the changes in the spectrum and the spatiotemporal distribution of the pulse intensity by varying the initial phase modulation and radiation wavelength.

## 2. Methods

The experimental scheme relied on a TOPAS tunable parametric amplifier combined with a Spitfire Pro regenerative amplifier. We used pulsed radiation at wavelengths of 800, 1300, 1800 and 1900 nm, which belong to the regions of normal, zero and anomalous dispersion in fused silica. At a wavelength of 800 nm, the FWHM of transform-limited pulses was 50 fs, the beam diameter at the waist was equal to about 100 μm, and the energy was varied from 1 to 15 μJ. The tuning of the output compressor enabled the phase modulation of 800-nm pulses over a wide range at which their durations increased up to 1000 fs. To change the phase modulation of femtosecond pulses with a centre wavelength in the near-IR range (1300–1900 nm), we used a specially designed (two-pass)

**S.V. Chekalin, V.O. Kompanets** Institute of Spectroscopy, Russian Academy of Sciences, ul. Fizicheskaya 5, 142190 Troitsk, Moscow, Russia; e-mail: chekalin@isan.troitsk.ru, kompanetsvo@isan.troitsk.ru;
**E.O. Smetanina, A.I. Spirkov, V.P. Kandidov** Department of Physics, M.V. Lomonosov Moscow State University, Vorob'evy gory, 119991 Moscow, Russia; e-mail: smetanina@physics.msu.ru, spirkov@physics.msu.ru, kandidov@physics.msu.ru

Received 3 March 2014; revision received 24 March 2014
Kvantovaya Elektronika **44** (6) 577–584 (2014)
Translated by I.A. Ulitkin

scheme of a reflective diffraction grating stretcher/compressor. To minimise losses when working with high power pulses, the scheme uses a small number of optical elements: a 600-lines $mm^{-1}$ diffraction grating with an efficiency of over 85% in the range of 1.25–3.2 μm and mirror elements with a reflectance of 96%. The scheme designed allows both positive and negative phase modulation in the range from 100 to 600 fs of pulse duration with a centre wavelength of 1300–1900 nm. In this case, the grating displacement constitutes several hundred micrometers, which enables the use of the desired phase modulation of the output radiation with sufficient accuracy. Phase-modulated radiation was focused by a thin quartz lens with a focal length of 50 cm on the input face of a fused silica sample in the form of an acute wedge [22]. The quartz lens had a thickness of 0.5 mm and did not distort the spectral composition of radiation. By moving the wedge in the direction perpendicular to the direction of radiation propagation, we varied the length of nonlinear-optical interaction of radiation in the fused silica sample. The applicable range of these lengths was 1–4 cm.

Recombination radiation of the laser plasma in the filament and conical emission of radiation scattered in the sample were recorded through the side face by a Canon EOS 450 digital camera. This gave information about the location and length of the regions of highest optical field intensity in the filament and therefore the regions of supercontinuum generation. The rings of conical emission in the far zone were observed on a screen at a distance of 50 cm from the output facet of the sample. To record the frequency-angular spectrum of the supercontinuum, broadband radiation at the output from the fused silica sample was collected by an achromatic lens, at the focus of which was the entrance slit of the monochromator. At the exit from the monochromator a CCD-camera measured the frequency-angular distribution of the supercontinuum components [22]. To find the autocorrelation functions of radiation during filamentation of pulses in the anomalous-GVD regime, the paraxial part of the filament at the sample output was separated by a diaphragm and collected by a parabolic mirror at the input window of the ASF-20 autocorrelator [6, 7].

The spatiotemporal transformation of the pulse during filamentation in fused silica was modelled numerically by using the slowly varying envelope approximation [23]. In the moving coordinate system the equation for the complex envelope of radiation, $A(r,t,z)$ at the carrier frequency $\omega_0$ under conditions of axial symmetry has the form

$$2ik_0\frac{\partial A}{\partial z} = \hat{T}^{-1}\Delta_\perp A + \int_{-\infty}^{\infty}\frac{1}{1+\Omega/\omega_0} \times [k^2(\omega_0+\Omega)-(k_0+k_1\Omega)^2]\tilde{A}(r,\Omega,z)\exp(i\Omega t)\,d\Omega + \frac{2k_0^2}{n_0}\hat{T}(\Delta n_K A) + \frac{2k_0^2}{n_0}\hat{T}^{-1}(\Delta n_p A) - ik_0\alpha A, \quad (1)$$

where $\tilde{A}(r,\Omega,z)$ is the time Fourier transform of the envelope; $k_0 = 2\pi/\lambda_0$; and $\Omega = \omega - \omega_0$ is the frequency shift of a supercontinuum harmonic. The dependence $k(\omega) = \omega n(\omega)/c_0$ and the parameter $k_1 = \partial k/\partial\omega|_{\omega=\omega_0}$ together with the function $n(\omega)$ approximated by the Sellmeier equation [24] describe the material dispersion in fused silica. The operator

$$\hat{T} = 1 - \frac{i}{\omega_0}\frac{\partial}{\partial t}$$

allows one to reproduce the wave nonstationarity during the pulse self-modulation, which manifests itself in increasing the steepness of its trailing edge and in forming a shock wave envelope [25]. The refractive index increment $\Delta n_K(r,t,z)$, due to the Kerr nonlinearity of the medium, in the approximation of an instantaneous response of electrons is described by

$$\Delta n_K(r,t,z) = n_2 I(r,t,z), \quad (2)$$

where $n_2 \approx 3.54\times10^{-16}$ $cm^2$ $W^{-1}$ is the Kerr nonlinearity coefficient for quasi-stationary radiation [26], and $I(r,t,z)$ is the optical field intensity. The refractive index increment in the induced laser plasma [27] reads

$$\Delta n_p(\boldsymbol{r},t,z) = -\frac{4\pi e^2 N_e(\boldsymbol{r},t,z)}{2n_0 m(\omega_0^2+\nu_c^2)}\left(1+\frac{i\nu_c}{\omega_0}\right), \quad (3)$$

where $n_0 \approx 1.45$ is the refractive index of fused silica; $\nu_c \approx 10^{14}$ $s^{-1}$ is the rate of electron–ion collisions; and $m = 0.64\,m_e$ is the reduced mass of the electron–hole pair. The concentration of free electrons in a laser plasma, $N_e$, obeys the kinetic equation

$$\frac{\partial N_e}{\partial t} = W(I)(N_0 - N_e) + \nu_i N_e, \quad (4)$$

where $N_0$ is the concentration of neutral atoms (for fused silica $N_0 = 2\times10^{22}$ $cm^{-3}$). The rate of field ionisation, $W(I)$, is defined by Keldysh's formula [28]. The avalanche ionisation frequency reads

$$\nu_i = \frac{e^2|A|^2}{2U_i m_e(\omega_0^2+\nu_c^2)}\nu_c. \quad (5)$$

The bandgap for fused silica is $U_i \approx 9$ eV. For radiation at $\lambda_0 = 800$ nm with an intensity $I \sim 10^{14}$ W $cm^{-2}$ typical of filamentation the frequency is $\nu_i \approx 10^{15}$ $s^{-1}$, and the avalanche ionisation contributes significantly to an increase in the electron density during the pulse. Equation (4) does not take into account recombination of electrons, whose characteristic time is a few hundreds of femtoseconds. The attenuation coefficient of the optical field in (1) reads

$$\alpha = \frac{K\hbar\omega_0}{I}W(I)(N_0 - N_e), \quad (6)$$

where $K = U_i/(\hbar\omega_0) + 1$ is the multiphoton order of the ionisation process.

In the experiments, the sample was placed at the waist of the beam focused by a long-focus lens, which allowed the plane-wave approximation for input radiation to be used in the mathematical modelling. Radiation on the input face of the sample was specified in the form of a collimated Gaussian beam with a Gaussian distribution of the field amplitude in time:

$$A(r,t,z=0) = A_0\sqrt{\tau_0/\tau_p}\exp\left(-\frac{r^2}{2a_0^2}-\frac{t^2}{2\tau_p^2}+\frac{i\delta t^2}{2}\right), \quad (7)$$

where $a_0$ is the beam radius; and $\tau_0$ and $\tau_p$ are the transform-limited and phase-modulated pulse half-durations at the $e^{-1}$ level. The parameters $\tau_0$ and $\tau_p$ are related with FWHM durations $\tau_{FWHM0}$ and $\tau_{FWHMp}$ of the corresponding pulses by the expression $\tau_{FWHM0(p)} = 2\sqrt{\ln 2}\,\tau_{0(p)}$. The phase modulation

parameter $\delta$ is expressed in terms of the parameters $\tau_0$ and $\tau_p$ as follows:

$$\delta = \pm \frac{\sqrt{(\tau_p/\tau_0)^2 - 1}}{\tau_p^2}, \quad (8)$$

where the sign '+' corresponds to a positive phase modulation, and the sign '–' – to a negative one.

The characteristic parameter of a change in the duration of a chirped pulse in a dispersive medium is the pulse compression length $L_{compr} = -(\tau_p^2\tau_0^2/k_2)\delta$, at which the pulse of duration $\tau_p$, having an initial negative temporal phase modulation ($\delta < 0$) in a medium with normal dispersion ($k_2 > 0$), will reach the duration $\tau_0$ and become transform-limited.

By solving numerically the system of equations for the optical field amplitude and the electron density in an induced laser plasma we determined the spatiotemporal distributions of the complex optical field amplitude, $A(r,t,z)$, and intensity, $I(r,t,z)$, of a femtosecond pulse during filamentation in fused silica for the experimental parameters. The angular-frequency spectra $S(\theta,\lambda)$ were calculated by the Fourier transform of the complex amplitude $A(r,t,z)$. In addition, for comparison with the experiment, the numerical spectra $S_{num}(\theta,\lambda)$ were calculated by taking into account the spectral sensitivity of the CCD-camera used in the experimental measurement of the frequency-angular spectra [22].

## 3. Normal GVD ($\lambda_0$ = 800 nm). Generation of a focused supercontinuum and conical emission in the Stokes region

Transformation of a supercontinuum frequency-angular spectrum during self-channelling of pulsed radiation at $\lambda_0 = 800$ nm in fused silica was studied as a function of the magnitude and sign of phase modulation. In fused silica this wavelength lies in the region of normal GVD ($k_2 \approx 360$ fs$^2$ cm$^{-1}$). In the case of phase modulation the pulse duration was increased from $\tau_{FWHM0} = 50$ fs ($\tau_0 = 30$ fs) to $\tau_{FWHMp} = 300$ fs ($\tau_p = 180$ fs). In fused silica the dispersion length $L_{disp} = \tau_0^2/k_2$ for such a transform-limited pulse was equal to 2.5 cm, and the pulse compression length with $\tau_{FWHMp} = 300$ fs in the case of negative phase modulation was $L_{compr} = 15$ cm. The laser energy $E$ remained unchanged and was 1.8 μJ. Under these conditions, the peak power $P$ decreased due to phase modulation from $17.5P_{cr}$ to $3P_{cr}$, where $P_{cr} = 1.87$ MW is a critical self-focusing power in fused silica for radiation with $\lambda_0 = 800$ nm. At a beam radius at the entrance face of the sample $a_0 = 50$ μm, the filament start distance, estimated by the Marburger–Talanov formula [29], increased from 0.3 to 1.2 cm.

When the pulse duration is increased by using phase modulation, the filament detected by the recombination luminescence in the plasma channel starts at a greater distance from the entrance face of the sample (Fig. 1), which corresponds to the above estimates. The blue glow of the plasma channel of the filament is the result of scattering of anti-Stokes supercontinuum emission in fused silica. It is seen that in a sample of fixed length, refocusing (recorded by formation of a second coaxial plasma channel in the filament) of phase-modulated pulses is absent. From a comparison of the frequency-angular spectrum of a transform-limited pulse (Fig. 1a) with the spectra in Figs 1b–1d it follows that when the pulse is phase modulated, the intensity of the spectral components of the supercontinuum conical emission in the anti-Stokes region decreases regardless of the sign of modulation. In this case, there appear divergent components of the spectrum in the Stokes wing of the supercontinuum, whose intensity increases with the duration of the phase-modulated pulse (Figs 1d–1g). Divergent Stokes components of the supercontinuum become significant after doubling the pulse duration under conditions of positive phase modulation and after its substantial increase under conditions of negative phase modulation (Figs 1f and 1g).

In laboratory and numerical experiments we found the emergence of focused broadband radiation in the anti-Stokes region upon filamentation under conditions of strong phase modulation corresponding to a seven- to ten-fold increase in the pulse duration (Figs 1f and 1 g). To explain this effect by numerical simulations, we compared in a wide range of frequencies and intensities of the spectral components the frequency-angular spectra of the supercontinuum generated during filamentation of transform-limited pulses of duration $\tau_{FWHM0} = 50$ and 400 fs at the same energy of 1.5 μJ. One can see from the frequency-angular spectra in Fig. 2 that a decrease in anti-Stokes component output power is not related to phase modulation.

Reduction in the intensity component of conical emission is caused by a decrease in the peak concentration of self-induced laser plasma and, hence, by a decrease in the slope of the trailing edge of the pulse. The peak electron density of the plasma channel of the filament, $N_{e\,max}$, for a 50-fs pulse reached $4.6\times10^{19}$ cm$^{-3}$, whereas during filamentation of a 150-fs chirped pulse it was $3.6\times10^{19}$ cm$^{-3}$ and in the process of filamentation of a 400-fs transform-limited pulse it decreased down to $3.1\times10^{19}$ cm$^{-3}$ (Fig. 3).

Flattening of the trailing edge of the pulse is illustrated in Fig. 4, which shows the time profiles of the intensity $I(t)$ when the intensity of the tail pulse reaches a maximum. The steepness of the trailing edge of a tail 'slow' subpulse is much higher than that of a 'fast' subpulse for the specified lengths of the pulse propagation. In this case, the sources of anti-Stokes components of the spectrum are mainly on the trailing edge of the 'slow' subpulse. The sources of conical emission of Stokes components are not presented in Fig. 4 because they are located in the annular radial structures of the intensity on the tail of the subpulse, appearing due to defocusing of radiation in the self-induced laser plasma. Reducing the concentration of self-induced laser plasma electrons leads to a decrease in the steepness of the trailing edge of the subpulse and intensity of annular radial structures formed during defocusing of radiation in the self-induced plasma and, consequently, to fall of the intensity of anti-Stokes components in the supercontinuum propagating along the axis and in the conical emission. A decrease in the intensity of anti-Stokes components as well as a reduction of the electron concentration in the laser plasma occurs with increasing the duration of the initial pulse, regardless of the presence or absence of phase modulation. The regions in the filament, where the supercontinuum is generated, coincide with plasma channels. As can be seen from Fig. 3, the length of these regions to the refocusing for each case varies insignificantly and the influence of their extent on the supercontinuum power in the anti-Stokes band is small.

We numerically calculated the evolution of the spatiotemporal distribution of intensity $I_{num}(r = 0,t,z)$ of femtosecond radiation at a wavelength of 800 nm with initial phase modulation. The distance $z$ travelled by the radiation in the medium is only a few centimetres, which exceeds the thickness of the sample in the experiments. Figure 5 shows the change in the temporal profile of the pulse, $I_{num}(r = 0,t,z)$, on the radiation

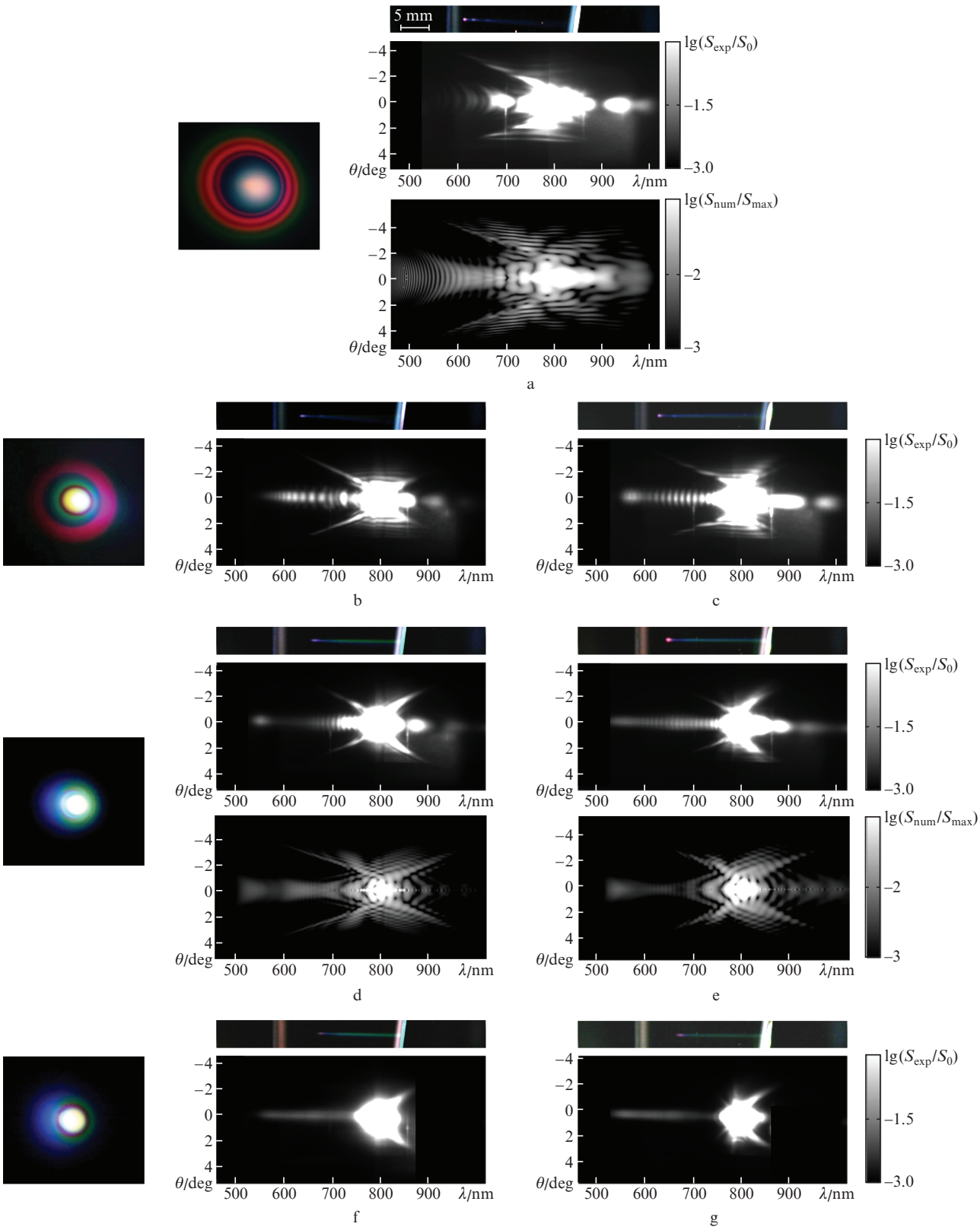


**Figure 1.** Experimentally recorded $[S_{exp}(0,\lambda)]$ and numerically obtained $[S_{num}(0,\lambda)]$ frequency-angular spectra of (a) transform-limited and (b–g) chirped pulses at $\lambda_0 = 800$ nm with (b, d, f) negative and (c, e, g) positive phase modulation during filamentation in fused silica at different pulse durations and peak powers: (a) $\tau_{FWHM0} = 50$ fs, $P \sim 18P_{cr}$; (b) $\tau_{FWHMp} = 120$ fs, $P \sim 7.5P_{cr}$; (c) $\tau_{FWHMp} = 100$ fs, $P \sim 9P_{cr}$; (d) $\tau_{FWHMp} = 290$ fs, $P \sim 3P_{cr}$; (e) $\tau_{FWHMp} = 200$ fs, $P \sim 4.5P_{cr}$; (f) $\tau_{TFWHMp} = 330$ fs, $P \sim 2.7P_{cr}$; and (g) $\tau_{FWHMp} = 300$ fs, $P \sim 3P_{cr}$. Above each experimental spectrum $S_{exp}(\theta,\lambda)$ there is a photograph which shows the plasma channels along the filament, the input and output faces of the sample (radiation propagates from left to right); to the left from the spectra shown are the photographs in the far zone of conical emission rings surrounding the white spot of the supercontinuum.

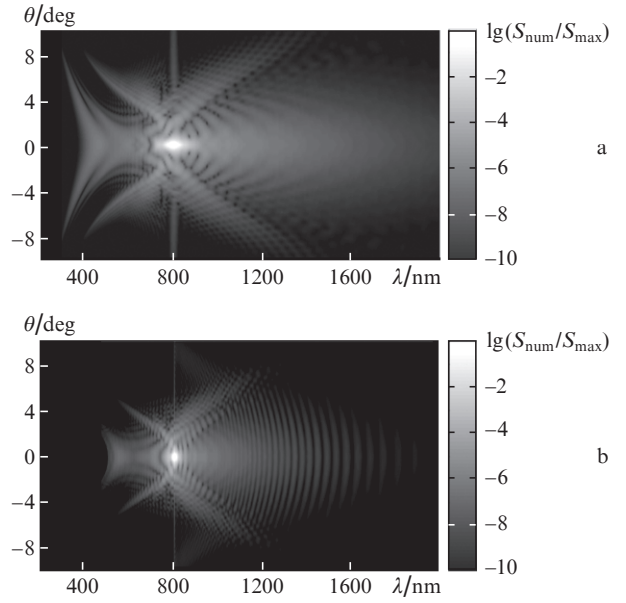


**Figure 2.** Frequency-angular spectra of supercontinuum during filamentation of a transform-limited pulse, obtained numerically at (a) $\tau_{FWHM0} = 50$ fs, $P \sim 15P_{cr}$ and (b) $\tau_{FWHM0} = 400$ fs, $P \sim 2P_{cr}$ for the beam radius at the entrance to the medium, $a_0 = 70$ μm.

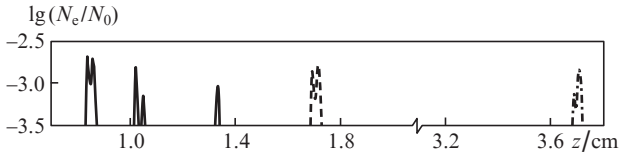


**Figure 3.** Concentrations of a self-induced laser plasma of a filament, obtained numerically for a transform-limited pulse with $\tau_{FWHM0} = 50$ fs, $P \sim 15P_{cr}$ (solid curves), a positively chirped pulse with $\tau_{FWHMp} = 150$ fs, $P \sim 5P_{cr}$ (dashed curve) and a transform-limited pulse with $\tau_{FWHM0} = 400$ fs, $P \sim 2P_{cr}$ (dot-dashed curve) for the beam radius at the entrance to the medium, $a_0 = 70$ μm, and the density of neutral atoms, $N_0 = 2.1\times10^{22}$ cm$^{-3}$.

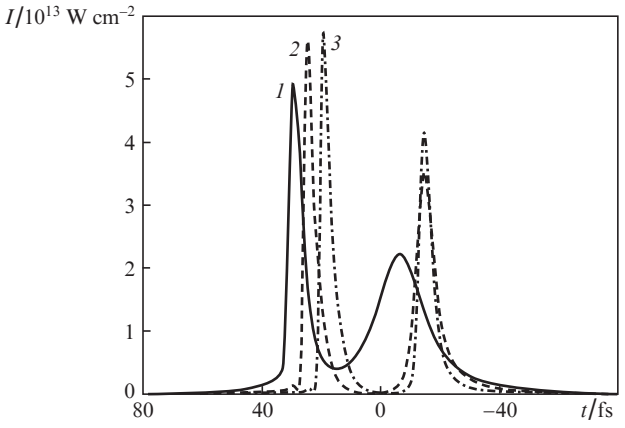


**Figure 4.** Time profiles of intensity $I(t)$ when the intensity of the tail subpulse reaches a maximum value, obtained numerically for (*1*) a transform-limited pulse with $\tau_{FWHM0} = 400$ fs, $P \sim 2P_{cr}$, (*2*) a positively chirped pulse with $\tau_{FWHMp} = 150$ fs, $P \sim 5P_{cr}$ and (*3*) a transform-limited pulse with $\tau_{FWHM0} = 50$ fs, $P \sim 15P_{cr}$ at $a_0 = 70$ μm. Negative values of time $t$ correspond to the leading edge of the pulse.

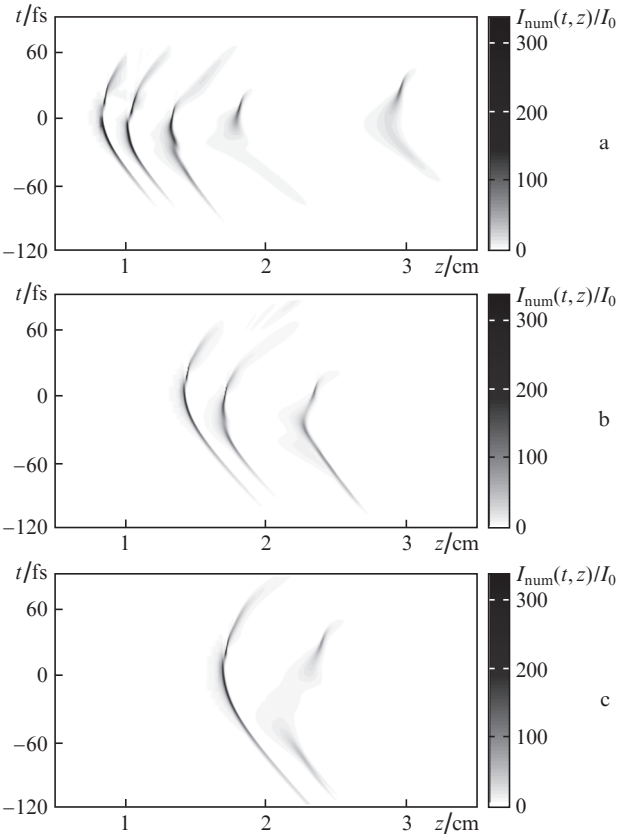


**Figure 5.** Transformation of intensity $I_{num}(r=0,t,z)$ on the beam axis ($\lambda_0 = 800$ nm) during filamentation of (a) a transform-limited pulse with $\tau_{FWHM0} = 50$ fs, $P \sim 15P_{cr}$ and pulses with (b) negative and (c) positive phase modulation with $\tau_{FWHMp} = 150$ fs, $P \sim 5P_{cr}$ in fused silica at $I_0 = 1.77\times10^{11}$ W cm$^{-2}$.

axis ($r = 0$) with increasing $z$. For each selected distance $z$, the vertical slice of the tone pattern, $I_{num}(t,z)$, represents a temporal pulse profile, $I_{num}(t)$.

In the case of initial phase modulation of radiation and constant energy, the distance to the formation of a nonlinear focus and refocusings increases as compared with the case of transform-limited radiation. Therefore, in experiments with a sample of thickness ~1.5 cm we failed to observe refocusing of phase-modulated pulses. For pulses of equal duration the distance between refocusings in the case of positive phase modulation is greater than that in the case of negative phase modulation. This is a consequence of an increase in the peak power when the pulse with a negative chirp is compressed under conditions of normal dispersion. In the case of weak refocusing of a phase-modulated pulse, the 'fast' subpulse at the leading edge of the pulse reaches its peak intensity at a smaller distance $z$, than the 'slow' subpulse located in the tail temporal slices of the pulse (Fig. 5).

Thus, this study showed that phase modulation of radiation does not alter the basic properties of spatiotemporal dynamics of the pulse during filamentation under conditions of normal GVD.

## 4. Zero GVD ($\lambda_0 = 1300$ nm)

For emission at $\lambda_0 = 1300$ nm in fused silica the dispersion parameter $k_2 = -23$ fs$^2$ cm$^{-1}$ should be an order of magnitude smaller in modulus than for emission at $\lambda_0 = 800$ nm, which

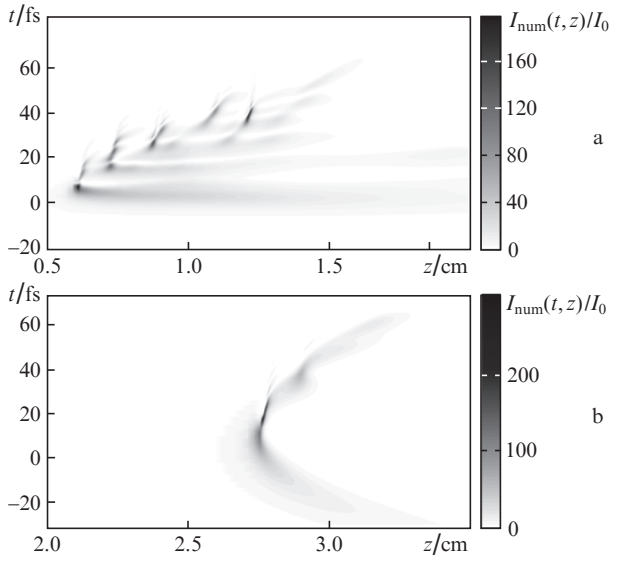


**Figure 6.** Transformation of the pulse profile, $I_{num}(r=0,t,z)$ on the beam axis ($\lambda_0 = 1300$ nm) during filamentation of (a) a transform-limited pulse with $\tau_{FWHM0} = 30$ fs, $P = 12P_{cr}$ and (b) a positively chirped pulse with $\tau_{FWHMp} = 200$ fs ($\tau_{FWHM0} = 30$ fs), $P = 2P_{cr}$ under conditions of zero GVD in fused silica at $E = 2.1$ μJ, $a_0 = 80$ μm, $I_0 = 3\times10^{11}$ W cm$^{-2}$ and $P_{cr} = 4.95$ MW.

leads to a significant reduction in the second-order dispersion influence and allows one to consider the propagation of radiation at $\lambda_0 = 1300$ nm in fused silica as a zero GVD regime. In the process of radiation filamentation at this wavelength the evolution scenario of the spatiotemporal intensity distribution significantly depends on the phase modulation of radiation. In terms of both positive and negative phase modulations, when the duration of a transform-limited pulse is at least twice the initial value, continuous refocusings of the pulse tail, which are typical of zero GVD (Fig. 6a), undergo a transition into a regime characteristic of normal GVD, in which the pulse splits into two subpulses (Fig. 6b) [5].

Along with the change in the evolution of the spatiotemporal intensity distribution of the phase-modulated pulses during filamentation under conditions of zero GVD the frequency-angular spectrum of the generated supercontinuum changes qualitatively. The so-called fish-shaped shape of the spectrum, which is characteristic of zero GVD, is transformed in the presence of phase modulation into a superposition of X- and fish- shaped forms (Fig. 7). The shape of the spectrum as a superposition of the X- and fish-shaped forms in the case of a transform-limited pulse is typical for a region of weak normal GVD during filamentation, for example, of radiation pulses at a wavelength of 800 nm in fused silica [22, 30].

## 5. Anomalous GVD ($\lambda_0 = 1900$ nm)

Filamentation under conditions of anomalous GVD of pulsed radiation at $\lambda_0 = 1900$ nm in fused silica ($k_2 = -801$ fs$^2$ cm$^{-1}$) is stable to both sign and magnitude of initial phase modulation. A train of light bullets is generated during filamentation of both a transform-limited pulse (Fig. 8a) and a phase-modulated pulse (Fig. 8b). The shape of the frequency-angular spectrum is qualitatively unchanged and in the case of anomalous GVD has an O-shaped form during filamentation of transform-limited and phase-modulated pulses (Fig. 9).

Formation of light bullets during filamentation under anomalous GVD of phase-modulated pulses was recorded experimentally by measuring the autocorrelation function of radiation, $J^{exp}_{corr}(t)$, in the aperture of 100 μm in diamter, mounted on the output face of the sample. With increasing energy $E$ of 1800-nm pulsed radiation with positive phase

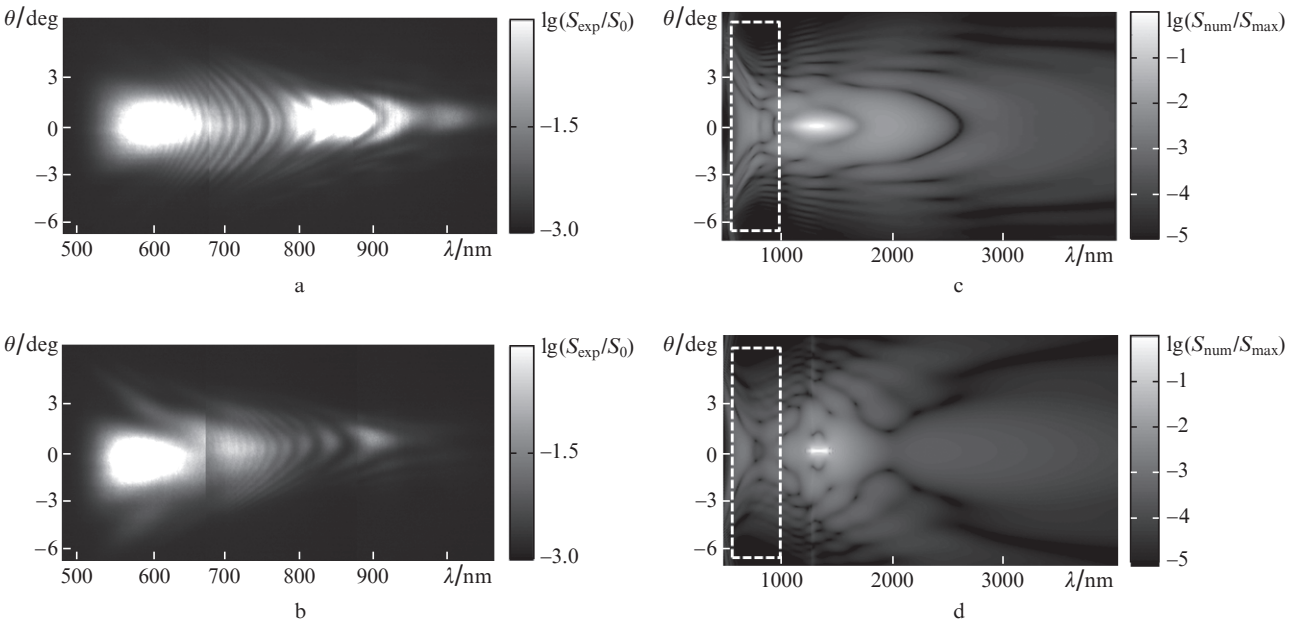


**Figure 7.** (a, b) Experimental and (c, d) numerically obtained frequency-angular spectra during filamentation of (a, c) transform-limited radiation and (b, d) radiation with positive phase modulation at a wavelength $\lambda_0 = 1300$ nm for (a) $\tau_{FWHM0} = 100$ fs, $E = 3$ μJ, (b) $\tau_{FWHMp} = 200$ fs ($\tau_{FWHM0} = 100$ fs), $E = 3$ μJ, (c) $\tau_{FWHM0} = 30$ fs, $E = 2.1$ μJ and (d) $\tau_{FWHMp} = 200$ fs ($\tau_{FWHM0} = 30$ fs), $E = 2.1$ μJ under conditions of zero GVD in fused silica at $a_0 = 80$ μm. White dashed rectangles show the region corresponding to the experimentally recorded spectrum.

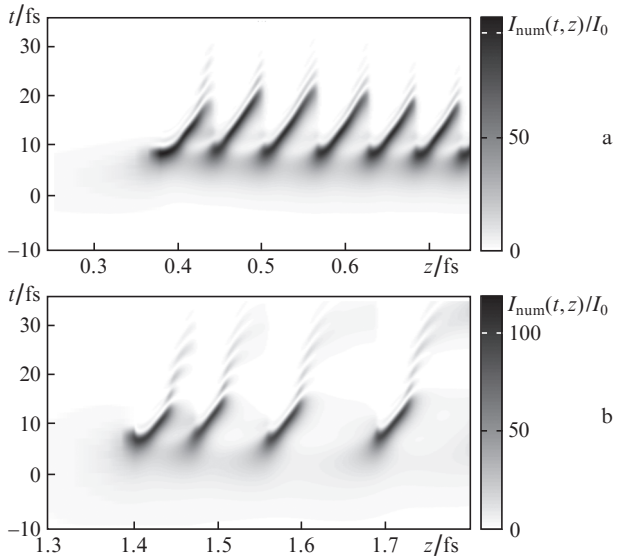


**Figure 8.** Transformation of intensity $I_{num}(r=0,t,z)$ on the beam axis ($\lambda_0$ = 1900 nm) during filamentation of (a) a transform-limited pulse with $\tau_{FWHM0}$ = 30 fs, $P = 10P_{cr}$ and (b) a positively phase modulated pulse with with $\tau_{FWHMp}$ = 200 fs ($\tau_{FWHM0}$ = 30 fs), $P = 1.7P_{cr}$ under conditions of anomalous GVD in fused silica at $E$ = 3.8 μJ, $a_0$ = 80 μm, $I_0 = 5.3\times10^{11}$ W cm$^{-2}$ and $P_{cr}$ = 10.6 MW.

modulation the peak value of the autocorrelation function $J^{exp}_{corr}(t)$ increases, while its duration decreases, reaching an extremum at $E$ = 11 μJ, which indicates the formation of the first light bullet at the exit from the sample at this energy (Fig. 10). The minimum width of the autocorrelation function $J^{exp}_{corr}(t)$ is 150 fs. With a further increase in the pulse energy the peak value of $J^{exp}_{corr}(t)$ decreases and its width increases. At $E$ = 13.5 μJ for a pulse with positive phase modulation the function $J^{exp}_{corr}(t)$ increases again and acquires a three-humped structure, which indicates the appearance of the second light bullet, existing simultaneously with the first one (Fig. 10). Formation of a train of light bullets under conditions of anomalous GVD during filamentation of a pulse with positive phase modulation has the same properties as in the case of a transform-limited pulses [6, 7].

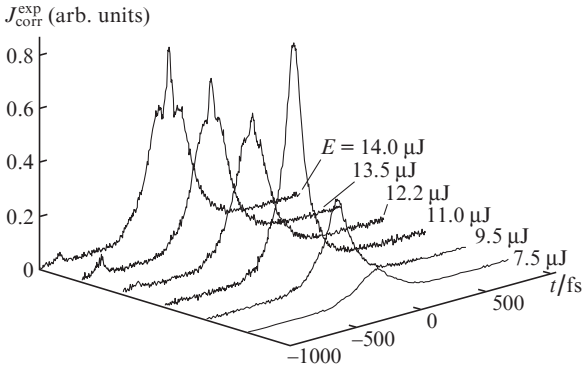


**Figure 10.** Experimentally recorded train of light bullets during filamentation in fused silica under conditions of anomalous dispersion of positively phase-modulated radiation at a wavelength of $\lambda_0$ = 1800 nm for $\tau_{FWHMp}$ = 210 fs (the width of the autocorrelation function, 300 fs; $\tau_{FWHM0}$ = 100 fs) and $a_0$ = 80 μm. The sample length is 2 cm, and the diameter of the selecting aperture is 100 μm.

## 6. Conclusions

Based on the experimental and numerical studies we have obtained general properties governing a change in the spatio-temporal intensity distribution and the frequency-angular spectrum of a femtosecond laser pulse during self-channelling in a condensed medium under conditions of initial phase modulation.

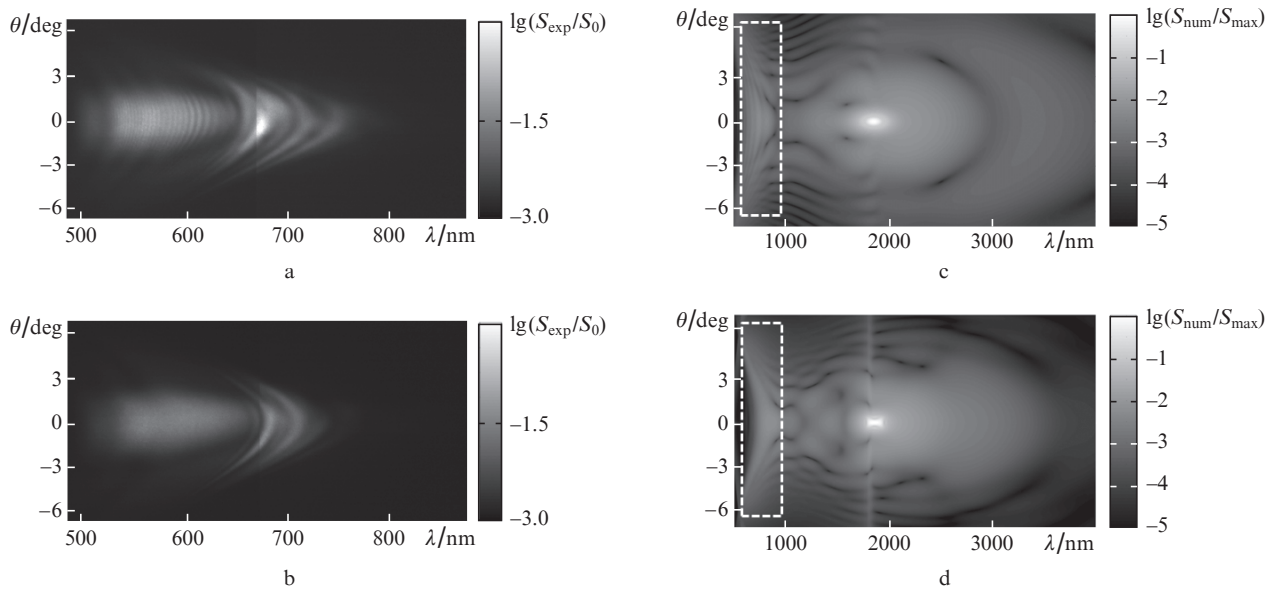


**Figure 9.** (a, b) Experimental and (c, d) numerically obtained frequency-angular spectra during filamentation of (a, c) transform-limited radiation and (b, d) radiation with positive phase modulation at a wavelength $\lambda_0$ = 1900 nm for (a) $\tau_{FWHM0}$ = 170 fs, $E$ = 4.4 μJ, (b) $\tau_{FWHMp}$ = 330 fs ($\tau_{FWHM0}$ = 170 fs), $E$ = 4.4 μJ, (c) $\tau_{FWHM0}$ = 30 fs, $E$ = 3.7 μJ and (d) $\tau_{FWHMp}$ = 200 fs ($\tau_{FWHM0}$ = 30 fs), $E$ = 3.7 μJ under conditions of anomalous GVD in fused silica at $a_0$ = 80 μm. White dashed rectangles show the region corresponding to the experimentally recorded spectrum.

We have found that in the process of filamentation under conditions of normal GVD, the presence of linear phase modulation does not change the spatiotemporal regime of radiation transformation, i.e., the pulse splits into two subpulses with group velocities different from the group velocity of initial radiation. During filamentation of both transform-limited and phase-modulated pulses of subpicosecond duration under conditions of normal GVD, there occurs a significant reduction in the intensity of anti-Stokes components of conical supercontinuum emission, resulting in the formation of focused broadband anti-Stokes radiation in the spectrum. Under conditions of zero GVD, when radiation is phase modulated, the regime of continuous refocusings of the pulse tail, which is characteristic of such GVD, is replaced by the regime characteristic of normal GVD at which the pulse splits into subpulses. The shape of the spectrum of a phase-modulated pulse during filamentation under conditions of zero GVD is a superposition of X- and fish-shaped forms. Under conditions of anomalous GVD, phase modulation does not affect the filamentation regime. A train of light bullets is formed in the filament of both a phase-modulated and a transform-limited pulse.

***Acknowledgements.*** This research was supported by the Presidium of the Russian Academy of Sciences (Extreme Light Fields and Their Applications Programme).

## References

1. Chin S.L., Hosseini S.A., Liu W., Luo Q., Theberge F., Akozbek N., Becker A., Kandidov V., Kosareva O., Schroeder H. *Can. J. Phys.*, **83**, 863 (2005).
2. Couairon A., Mysyrowicz A. *Phys. Rep.*, **441**, 47 (2007).
3. Kandidov V.P., Shlenov S.A., Kosareva O.G. *Kvantovaya Elektron.*, **39**, 205 (2009) [*Quantum Electron.*, **39**, 205 (2009)].
4. Skupin S., Berge L. *Physica D*, **220**, 14 (2006).
5. Smetanina E.O., Dormidonov A.E., Kandidov V.P. *Laser Phys.*, **22** (7), 1189 (2011).
6. Smetanina E.O., Kompanets V.O., Dormidonov A.E., Chekalin S.V., Kandidov V.P. *Laser Phys. Lett.*, **10**, 105401 (2013).
7. Chekalin S.V., Kompanets V.O., Smetanina E.O., Kandidov V.P. *Kvantovaya Elektron.*, **43**, 326 (2013) [*Quantum Electron.*, **43**, 326 (2013)].
8. Wille H., Rodriguez M., Kasparian J., Mondelain D., Yu J., Mysyrowicz A., Sauerbrey R., Wolf J.P., Wöste L. *Eur. Phys. J. Appl. Phys.*, **20**, 183 (2002).
9. Golubtsov I.S., Kandidov V.P., Kosareva O.G. *Kvantovaya Elektron.*, **33**, 525 (2003) [*Quantum Electron.*, **33**, 525 (2003)].
10. Nuter R., Skupin S., Bergé L. *Opt. Lett.*, **30** (8), 917 (2005).
11. Kasparian J., Sauerbrey R., Mondelainet D., et al. *Opt. Lett.*, **25** (18), 1397 (2000).
12. Kasparian J., Rodriguez M., Mejean G., et al. *Science*, **301** (5629), 61 (2003).
13. Polynkin P., Kolesik M., Moloney J. *Opt. Express*, **17** (2), 575 (2009).
14. Yang J.J., Yang Y., Wang R., Han W. *Sci. China, Ser. E: Technol. Sci.*, **51** (7), 849 (2008).
15. Park J., Lee J., Nam C.H. *Opt. Express*, **16** (7), 4465 (2008).
16. Hauri C.P., Guandalini A., Eckle P., Kornelis W., Biegert J., Keller U. *Opt. Express*, **13** (19), 7541 (2005).
17. Shlenov S.A., Fedorov V.Yu., Kandidov V.P. *Opt. Atmos. Okean.*, **20** (4), 308 (2007).
18. Fedorov V.Yu., Shlenov S.A., Kandidov V.P. *Eur. Phys. J. D*, **50**, 185 (2008).
19. Panov N.A., Kosareva O.G., Kandidov V.P., Akosbek N., Skalora M., Chin S.L. *Kvantovaya Elektron.*, **37**, 1153 (2007) [*Quantum Electron.*, **37**, 1153 (2007)].
20. Borzsonyi A., Heiner Z., Kalashnikov M.P., Kovács A.P., Osvay K. *Appl. Opt.*, **47** (27), 4856 (2008).
21. Wrzesinski P.J., Pestov D., Lozovoy V.V., Gord J.R., Dantus M., Roy S. *Opt. Express*, **19** (6), 5163 (2011).
22. Kandidov V.P., Smetanina E.O., Dormidonov A.E., Kompanets V.O., Chekalin S.V. *Zh. Eksp. Teor. Fiz.*, **140**, 484 (2011).
23. Brabec T., Krausz F. *Phys. Rev. Lett.*, **78**, 3282 (1997).
24. Malitson I.H. *J. Opt. Soc. Am.*, **55**, 1205 (1965).
25. Akhmanov S.A., Vysloukh V.A., Chirkin A.S. *Optics of Femtosecond Laser Pulses* (New York: American Institute of Physics, 1992; Moscow: Nauka, 1988).
26. Kelley P.L., Kaminov I.P., Agraval G.P. *Nonlinear Fiber Optics* (New York: Academic Press, 2001).
27. Raiser Yu.P. *Gas Discharge Physics* (New York: Springer, 1991; Moscow: Nauka, 1992).
28. Keldysh L.V. *Zh. Eksp. Teor. Fiz.*, **47**, 1945 (1964).
29. Chekalin S.V., Kandidov V.P. *Usp. Fiz. Nauk*, **183**, 133 (2013).
30. Dormidonov A.E., Kandidov V.P. *Laser Phys.*, **19** (10), 1993 (2009).